Proceedings Paper:

Mixture Reactivity Effects on Explosion Venting

Fakandu, B.[a], Kasmani, R.M.[b], Phylaktou, H.N.[c], Andrews, G.E.[c]

E-mail: profgeandrews@hotmail.com

[a] Nigerian Military Academy, Nigeria
[b] Faculty of and Renewable Energy, Petroleum Universiti Teknologi Malaysia, Johor
[c] School of Chemical and Process Engineering, University of Leeds, Leeds, LS2 9JT, UK

Keywords: venting, industrial explosions, methane, propane, ethylene, hydrogen

Abstract

Free vented explosions were investigated for 10% methane, 4.2 and 4.5% propane, 6.5 and 7.5% ethylene, 30% and 40% hydrogen in a 10 litre cylindrical explosion vessel for vent coefficients of 4.3 and 21.7. The cylindrical vessel volume was 10L and had a diameter of 162mm and an L/D of 2.8. End ignition was used on the wall opposite the vent. The results are presented against K_G and the laminar burning velocity as measures of the mixture reactivity. It is shown that the correlation of the K_G effect by Bartknecht does not agree with other experimental data, although the hydrogen results are closer to the present results than the other gases. In contrast the laminar flame venting theory, as used in NFPA68 (2013), does correlate the data well, even though it is not supposed to apply to hydrogen explosions. There was evidence of very fast flames at the vent for hydrogen explosions. Acceleration of the flames towards the vent was demonstrated, due to the expansion of the burnt gases in the direction of the vent. The laminar flame venting theory that is used in NFPA68 (2013) over predicts the measured P_{red} due to the assumption of the vessel surface area as the area of the flame at P_{red}. It was shown that the flame arrives at the wall after the flame has vented the vessel and well after the time that P_{red} occurs. At K_v 4.3 the external overpressure was responsible for P_{red}, although the difference from P_{fv} was small for methane, propane and ethylene but for hydrogen the flow through the vent P_{fv} was the highest overpressure. At $K_v =$ 21.7 the pressure loss due to the unburnt gas flow through the vent was the largest overpressure. For hydrogen sonic flow at the vent occurs and at high K_v sonic flow is predicted to occur using the laminar flame venting equation modified for sonic flow at the vent. Sonic flow at the vent is not taken into account in current venting guidance.

Keywords: methane, propane, ethylene, hydrogen, mixture reactivity, venting

Introduction

12th International Symposium on Hazards, Prevention and Mitigation of Industrial Explosions
Kansas City, USA - August 12-17, 2018

XII ISHPMIE
Kansas City, MO August 12–17, 2018

The reduced overpressure, P_{red}, of any vented explosion depends on the reactivity of the mixture, the volume and shape of the vessel, the ignition position and the initial turbulence levels (Catlin, 1991, Hermanns et al., 2010, Hjertager, 1984, Phylaktou and Andrews, 1993, Razus and Krause, 2001). This complexity of influences on the venting of gaseous explosions led Hattwig and Steen (2004) to conclude that current knowledge does not permit satisfactory predictions of P_{red} for vented gas explosions. The reactivity of the mixture of gases is taken into account using either the laminar burning velocity, U_L, in NFPA68 (2013) or the deflagration parameter, $K_G = (dp/dt)_{max}V^{1/3}$ in EN14994:2007. Current gas explosion vent design standards are based on experimental results in empty compact vessels (L/D~1) with central ignition. NFPA 68 [2007] and EN14994:2007 [2007] use K_G as the reactivity parameter, but NFPA 68 [2013] has abandoned this approach and uses the laminar burning velocity, U_L, approach for mixture reactivity influences, up to a maximum of 3 m/s and for mixture concentrations <10%, which excludes hydrogen/air venting at the maximum reactivity composition (3.5 m/s U_L and 40% H_2 in air). No guidance is thus given in NFPA 68 2013 for hydrogen-air venting, but such guidance is given in EN14994:2007 which is the same guidance that used to be in NFPA 68 2007.

The laminar burning velocity was used in the laminar flame venting theory developed by Swift (1983, 1988) which was recognised in NFPA 68 [2007] and EN14994:2007 for low (<0.1 bar) P_{red} and in NFPA 68 [2013] for P_{red} up to 0.5 bar. The Swift [1988] methodology for higher overpressure with compressible flow at the vent was also used in NFPA68 2013, with no stated limitation on the maximum P_{red}. As sonic flow occurs at $P_{red} > \sim 0.9$ this must be the upper limit of applicability of the design approach in NFPA 68 2013. Sonic flow venting is not addressed in NFPA 68 2013, although for high initial pressures venting is sonic and vent design procedures are given for this, based on the sonic venting flow methodology of Epstein, Swift and Fauske [1986]. All theories of vented explosions [Bradley and Mitcheson, 1978a, b; Swift, 1983, 1988; Cates and Samuels, 1991; Molkov et al., 1999; Molkov et al., 2000; Bauwens et al., 2010; and Andrews and Phylaktou, 2010; Fakandu et al., 2016b] use the laminar burning velocity, U_L, as the reactivity parameter.

The K_G and U_L approaches to the inclusion of mixture reactivity in explosion venting design are directly related and can be interchanged. Andrews and Phylaktou [2010] derived Eq. 1 from spherical flame propagation theory. In a spherical vessel 98% of the pressure rise occurs in the second half of the flame travel distance. The chief approximation in the derivation of Eq. 1 is that U_L is assumed to be constant throughout the flame travel. This is not valid as for hydrocarbons as U_L decreases as pressure increases and increases as the unburned gas temperature increases due to compression. However, the computations of Bradley and Mitcheson [1976] show that this effect is a maximum change in U_L of 20% from the initial value for a spherical closed vessel explosion. A mean value of U_L 10% higher than that at ambient conditions would be reasonable in Eq. 1. However, there is no agreement on a standard method to determine U_L and published values vary widely, by much more than 10% [Andrews and Bradley, 1972].

$$K_G/P_i = [d(P/P_i)/dt]_{max}/V^{1/3} = 3.16 \, [P_m/P_i - 1]U_L E_p \quad \text{m/s} \qquad (1)$$

The flame speed, which governs the actual time taken to burn the unburnt gas mixture, is the burning velocity times the expansion ratio. In Eq. 1 the constant pressure combustion expansion ratio, E_p, has been used. It could be argued that in the final stages of combustion it is the temperature at high pressure that is more important in the expansion and hence the constant volume expansion ratio, E_v, should be used to determine the flame speed from the burning velocity. In this case Eq. 2 relates K_G and U_L. The expansion ratio at constant volume, E_V, is the ratio of peak pressure to initial pressure, as shown in Eq. 2.

$$K_G/P_i = 3.16 \ [P_m/P_i - 1] \ U_L E_v \ = \ 3.16 \ U_L \ [P_m/P_i - 1] \ [P_m/P_i] \ m/s \qquad (2)$$

Where P_m is the maximum adiabatic pressure (bara) in a closed spherical vessel.

P_i is the initial pressure (bara)

E_v is the unburned gas to burned gas density ratio or expansion ration at constant pressure

A very similar expression to that in Eq. 2 was also derived by Kumar et al. [1992] and Hattwig and Steen [2004] and this is shown in Eq. 3. This was derived from the theory of spherical flame propagation in a closed spherical vessel which gives the pressure rise as a function of the radius of the flame, differentiation of this to determine the maximum dP/dt then enables K_G to be predicted. Kumar et al. [1992] and Hattwig and Steen [2004] also assumed a constant burning velocity in the derivation of Eq. 3. The value for the ratio of specific heats, γ, in Eq. 3 is that for the unburnt gases and is close to that of air, which with some preheat is about 1.38. Eq. 2 is derived as the average rate of pressure rise from the first 2% pressure rise to peak pressure and Eq. 3 as the peak rate of pressure rise. In practice in real explosions there is little difference between the maximum and average, measured from the start of pressure rise.

$$K_G/P_i = 4.84 \ U_L \ [P_m/P_i - 1] \ [P_m/P_i]^{1/\gamma} \qquad (3)$$

Hattwig and Steen [2004] have suggested the approximation in Eq. 4 for the link between U_L and K_G, which is essentially a scaling function based on a U_L of 0.48 m/s for propane/air with $K_G/P_i = 100$ m/s, if the NFPA 68 accepted value of 0.46 m/s for propane is used instead then Eq. 4 becomes the relationship between K_G and U_L.

$$K_G/P_i = \sim 217 \ U_L \ m/s \qquad (4)$$

Eqs. 1 - 4 show that if the rate of pressure rise is normalised to the initial pressure then the deflagration parameter has units of m/s and is proportional to the laminar burning velocity, U_L. This form of K_G/P_i is preferred as it can be applied to any initial pressure.

The predictions of K_G/P_i from Eqs. 1-4 are compared in Table 1 with the measured values of K_G in a 5L sphere by Bartknecht [1993] and for a 1 m[3] vessel by the authors. The values for U_L are taken from NFPA 68 2013, which uses a reference value of 0.46m/s for propane-air taken from France and Pritchard [1977], so the U_L for methane (0.43 m/s) and hydrogen (3.50 m/s) have also been taken from France and Pritchard [1977]. The methane burning velocity of 0.43 m/s is close to measurement of 0.42 m/s in a 1 m[3] spherical vessel explosion by Satter et al. [2012]. The table of values for U_L for 117 gases in NFPA 68 2013 also gives 0.46 m/s as the maximum burning velocity for propane/air, in agreement with the data of Frances and Pritchard [1977]. However, the value for methane and propane in the burning velocity table in NFPA 68 is 0.4 and 3.12 m/s, which are inconsistent with the values from Francis and Pritchard [1977]. In this work the value of 0.8 m/s for the burning velocity of ethylene has been used from NFPA 68 2013.

Table 1 shows that Eq. 4 is too simplistic and takes no account of the influence of P_m/P_i on K_G, its values for methane and hydrogen from Eq. 4 are too high for both gases. Table 1 also shows that the Bartknecht [1993] K_G value of 55 for methane is far too small relative to the 100 bar m/s for propane, to be compatible with measured values of U_L for these gases. Cashdollar et al. [2000] have measured K_G for methane at 65 bar m/s in a 20L vessel (0.168m radius) and 90 bar m/s in a 120L vessel (0.306m radius), which gives an average value of 72 bar m/s. In NFPA 68 1988 other measurements of K_G than those of Bartknecht [1993] are reported with 64 bar m/s for methane, 96 for propane and 659 for hydrogen. All of these results and the present results measured in a 1m[3] vessel in Table 1 indicate that the 55 bar m/s

K_G for methane is too low and that a more reasonable value is in the range 70 - 90 bar m/s. This difficulty over a reliable K_G for methane makes comparison with Eqs. 1-3 difficult. However, if the K_G of 100 bar m/s is reliable for propane, and the same value was found by the authors in a 1m³ explosion vessel, then Eq. 1 or 3 could be judged as the most reliable relationship between U_L and K_G. However, Table 1 shows that Eqs. 1 and 3 give quite low values for hydrogen K_G and Eq. 2 gives the best agreement with measurements for hydrogen.

Table 1: Comparison of K_G/P_i Measurement and Predictions from U_L

Gas Maximum Reactivity Conc.	K_G/P_i m/s Bartknecht (1993) 5L sphere	K_G/P_i m/s 1 m³ This work	U_L m/s France & Pritchard 1977	E_v	E_p	E_v/E_p	Eq. 1 K_G/P_i m/s	Eq. 2 K_G/P_i m/s	Eq.3 K_G/P_i m/s γ= 1.38	Eq. 4 K_G/P_i m/s
Methane	55	72	0.43	8.85	7.54	1.17	80	94	79	93
Propane	100	102	0.46	9.53	8.05	1.18	100	118	97	100
Ethylene		220	0.95*							
Hydrogen	550 29%	693 40%	3.50	7.70	6.47	1.19	479	571	499	760

*This work, as in Fig. 3

Table 2: Comparison of K_G and U_L from NFPA 68 2013 data

Gas	K_G	$K_G/K_{G\ Propane}$	U_L	$U_L/U_{L\ propane}$
Propane	100	1.0	0.46	1.0
Methane	55	0.55	0.40	0.87
Methanol	75	0.75	0.56	1.22
Butane	92	0.92	0.45	0.98
Ethane	106	1.06	0.47	1.02
Pentane	104	1.04	0.46	1.00
Carbon disulphide	105	1.05	0.58	1.26
Diethyl Ether	115	1.15	0.47	1.02
Isopropanol	83	0.83	0.41	0.89
Toluene	94	0.94	41	0.89
Acetylene	1415	14.1	1.66	3.61
Hydrogen	550	5.5	3.12	6.78

Satter et al. [2014] have used the ISO 1 m³ dust explosion vessel for the simultaneous measurement of K_G and U_L by measuring the flame speed, S_s, in the constant pressure period of the explosions and deriving U_L from this. The simple $U_L = S_s/E_p$ is valid for large explosion vessels as the infinitely thin flame front assumption is valid if the vessel is large enough. The results for a range of gas reactivities is shown in Figure 1, which demonstrates a linear correlation between K_G and U_L, as predicted by Eqs. 1-4.

For compliance with the venting design guides using K_G to measure the mixture reactivity, the values of K_G experimentally measured in a 5L spherical vessel by Bartknecht [1993] have to be used, as the vent design equation is based on the work of Bartknecht [1993] and his values of K_G must be used if the original experimental vent overpressures are to be obtained. Unfortunately, these values of K_G do not correlate with U_L for all gases as is shown in Table 2. If the values of K_G and U_L relative to propane are compared then it can be seen that, of the 12 gases where NFPA 68 has both K_G and U_L data, there is agreement to within 10% of their
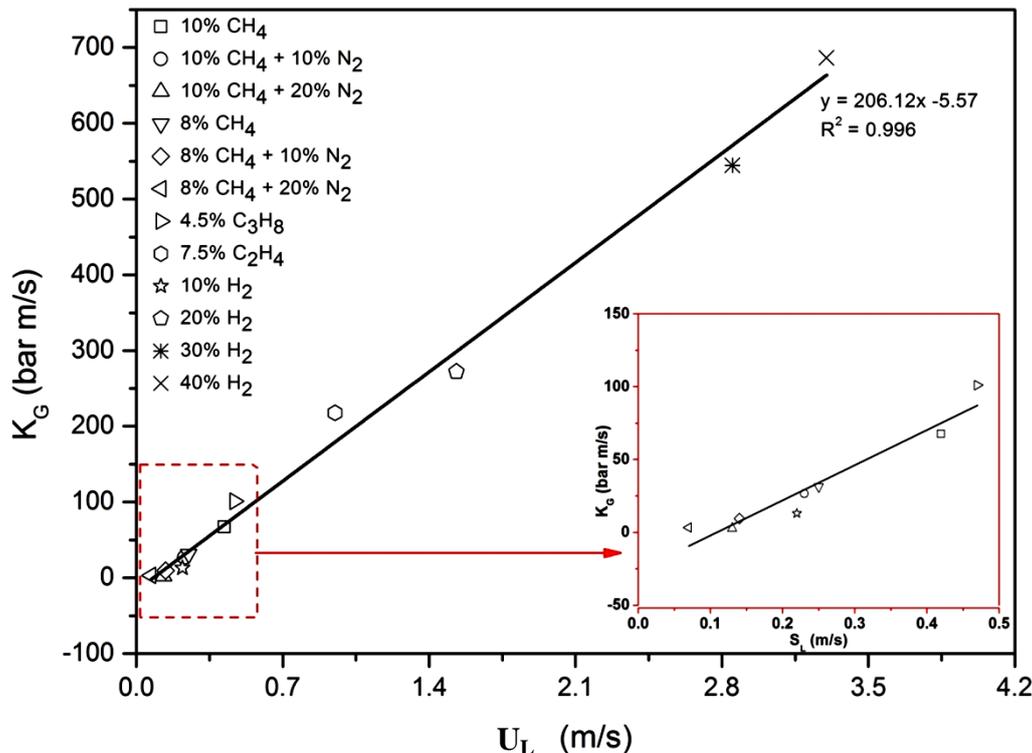
Figure 1: K_G v. U_L for both measurements made simultaneously in the ISO 1m^3 spherical dust explosion vessel

relative K_G and U_L. However, there are 5 gases that have widely different relative K_G and U_L and these include the common gases methane, methanol, acetylene and hydrogen as well as carbon disulphide. For U_L to be used in the design procedures for gas explosion venting for different mixture reactivities, then standardisation of the measurement method for U_L is required. Also standard values of the mixture reactivity in terms of K_G and U_L are required that show the same relative reactivity for all gases. Andrews and Bradley [1972] reviewed measurements of U_L and showed a strong dependence on the method of measurement, with many methods having systematic errors. Since then there has continued to be published U_L measurements, particularly for methane-air, with much the same variability as that reviewed in 1972.

There have been relatively few investigations of the influence of mixture reactivity on vent design and the current European design methodology is based on one set of vented explosion data [Bartknecht, 1993]. In the USA venting design procedures in NFPA 68 2013, the U_L approach to mixture reactivity is stated to be valid for U_L up to 3.0 m/s and yet there is minimal experimental venting data for mixtures significantly more reactive than propane, such as ethylene and acetylene, in spite of the extensive use of ethylene in the petrochemicals industry. There is concern that the current European design methodology is particularly in

12th International Symposium on Hazards, Prevention and Mitigation of Industrial Explosions
Kansas City, USA - August 12-17, 2018

XII ISHPMIE
Kansas City, MO August 12-17, 2018

error in relation to the venting of hydrogen explosions [Kasmani et al., 2010a, b]. The USA guidance in NFPA68 [2013] has no procedures that apply to hydrogen venting, as they do not apply for mixtures with more than 10% of the reactive gas in air or for U_L>3 m/s and both these criteria exclude hydrogen from the guidance, but include ethylene and acetylene. With the widespread use of hydrogen being advocated in energy generation, as a means to eliminate CO_2 emissions, more reliable hydrogen venting design guidance is required.

The present work presents vented explosion experimental data for the influence of mixture reactivity using methane, propane, ethylene and hydrogen-air (30% and 40%) vented explosions at two values of the vent coefficient K_v ($K_v = V^{2/3}/A_v$) for free venting. The use of K_v in gas explosion vent design equations, with no other term including the vessel volume, implies that the size of the vessel used in the venting experiments is not important. Nevertheless, many investigations of gas explosion venting have involved expensive experiments in very large vented vessels, closer to the vessel size required to have vent protection. This implies a lack of confidence that the K_v term does include all the influences of vessel volume. In the present work a very small 0.01 m^3 vessel was used for two purposes: firstly, to compare the results with experiments in large vessels at the same K_v to see if there was an additional volume effect and secondly, to produce experimental results where the assumption of laminar flames was valid, with negligible self acceleration of the flame due to the development of a cellular structure. Fakandu et al. [2016b] reviewed experimental vented data for methane and propane and compared it with the P_{red} from the present 10L vessel, this showed that there was a wide data scatter with no consistent volume effect and some large volume vessel experiments had similar P_{red} to the 10L vented vessel results.

2. Laminar Flame Venting Theory

Most theories of venting to date assume that flow through the vent, P_{fv}, dominates the overpressure [Bradley and Mitcheson, 1978 a, b; Swift, 1983; Cates and Samuel, 1991; [Molkov, 1999, 2000; Fakandu et al., 2016b]. The other main cause of the peak overpressure in vented explosions is the external explosion, P_{ext}, which occurs as the flame leaving the vent ignites the turbulent cloud of unburnt gas expelled from the vented vessel ahead of the flame. In the present work a thermocouple was located at the vent to enable these two overpressure peaks to be distinguished, with P_{ext} occurring after the flame left the vent. Fakandu et al. [2016a] have shown that the external explosion may be modelled as a turbulent explosion, using the vent blockage to the explosion to predict the mean turbulence level and the downstream flame speed. Measurements of the external flame speed were used to predict P_{ext} using Taylors equation [1946] and reasonable agreement was shown. However, the mass of unburnt gas expelled outside the vent is related to the mass flow rate of the unburnt gas through the vent, which is predicted by laminar flow venting theory. Also the turbulence in the unburnt gases downstream of the vent is also controlled by the mass flow through the vent. Thus the physics of the external explosion is related to that of the flow of unburnt gas through the vent. Fakandu et al. [2016b] have shown that for propane and methane vented explosions that P_{fv} controls the P_{red} for K_v >~10 and P_{ext} controls P_{red} for K_v<~10. However, P_{fv} and P_{ext} are similar for most K_v and it is only for K_v < 5 that P_{ext} is significantly higher than P_{fv}. Thus, understanding the factors that control P_{fv} is important as the same factors also control P_{ext} as they control the quantity of and the turbulence in the unburnt gas.

The classic laminar flame venting model [Bradley and Mitcheson, 1978a] assumes that a spherical flame in a spherical vessel with central ignition propagates uniformly until all the unburned mixture ahead of the flame is expelled through the vent. The maximum overpressure is then the vent orifice flow pressure loss at the maximum unburned gas vent mass flow rate [Andrews and Phylaktou, 2010]. The unburned gas mass flow rate is the flame

12th International Symposium on Hazards, Prevention and Mitigation of Industrial Explosions
Kansas City, USA - August 12-17, 2018

XII ISHPMIE
Kansas City, MO August 12–17, 2018

surface area, A_f, times the unburned gas velocity ahead of the flame, $U_L(E_p-1)$, times the unburned gas density, ρ_u. A further assumption is made that simplifies the theory and this is that the maximum possible flame area is the surface area of the vessel walls, A_s. This was an assumption first proposed by Runes [1972].

The laminar flame venting model with the above assumptions, leaves the prediction of P_{red} a function of A_v/A_s, as shown in Eq. 5. [Andrews and Phylaktou, 2010]. Bradley and Mitcheson [1978 a, b], Swift [1983, 1988] and Molkov [1999, 2000] all left the theoretical venting equation in terms of A_v/A_s and the Swift [1988] formulation of the laminar flame venting theory has been adopted in NFPA 68 2013. In the original Swift [1983] formulation of Eq. 6 a turbulence factor of 5 was assumed, but this has been replaced with λ and a procedure given in NFPA 68 2013 to calculate this.

$$A_v/A_s = C_1 \, \varepsilon^{-1} \, \lambda \, U_L \, (E_p-1) \; P_{red}^{-0.5} \quad \text{with } P_{red} \text{ in Pascals} \tag{5}$$

where $C_1 = \rho_u^{0.5}/(C_d \, 2^{0.5}) = 1.27$ for $\rho_u = 1.2$ kg/m^3 and the vent discharge coefficient $C_d = 0.61$. Fakandu et al. (2016b) have further developed Eq. 5 to take into account the variation of density, ρ_u, with P and T as P_{red} increases and the compressible flow term ε. These corrections are relatively small for $P_{red} < 0.5$ and do not affect the mixture reactivity influence on P_{red}.

With P_{red} in Eq. 5 converted to bar and the above value for C_1 inserted and an E_p of 8.05 used, which is the adiabatic value for propane, Eq. 5 becomes Eq. 6 for P_{red} in bar.

$$A_v/A_s = 0.0283 \, \varepsilon^{-1} \, \lambda \, U_L \, P_{red}^{-0.5} \tag{6}$$

The constant in Eq. 6 becomes 0.0247 if a C_d of 0.7 is used, as in the work of Swift [1983] which is the C_d value adopted in NFPA 68 2013 as Eq. 7. The predicted value of the constant in Eq. 6 with $C_d = 0.7$ is only 11% higher than Eq. 7 and so the laminar flame venting theories have very similar results.

$$A_v/A_s = C \, P_{red}^{-0.5} = 0.0223 \, \lambda \, U_L \, P_{red}^{-0.5} \quad \text{for } P_{red} < 0.5 \text{ bar} \tag{7}$$

There is no reason for limiting this equation to a P_{red} of 0.5 bar as all compressibility effects are contained in the expansibility factor, ε, in Eqs. 6 and 7. This shows that the present approach to the laminar flame venting theory produces a very similar vent design equation to that of Swift [1983] adopted in NFPA 68 2013.

It may also be shown that the laminar flame venting theory of Bradley and Mitcheson [1978a] for free venting can be expressed in the above format as in Eq. 8.

$$A_v/A_s = 0.831[\lambda \, U_L(E_p - 1)] / [C_d \, a_v \, P_{red}^{0.5}] = 0.0284 \, \lambda \, U_L \, P_{red}^{-0.5} \tag{8}$$

where a_v is the velocity of sound at the vent, taken as 343 m/s for air. E_p has been taken as the adiabatic value for propane of 8.05. Eq. 8 is identical to Eq. 6. There was a difference in C_d of 0.6 instead of 0.61 used in Eq. 10, but this only changes the constant in Eq. 8 to 0.0280. Bradley and Mitcheson (1978b) went on to use a value for the turbulence factor λ of 4.19 to produce a prediction that would encompass data from vented explosions with a static burst pressure at the vent. Eq. 8 also shows that the artificial dimensional numbers used by Bradley and Mitcheson, termed the Bradley number by Molkov [1999, 2000] are unnecessary, as the $0.0284 \, U_L$ term in Eq. 12 has units of bar$^{-0.5}$ so that Eq. 8 is dimensionless.

The A_v/A_s formulation of the laminar flame venting equation can be converted into a form using the vent coefficient K_v as $A_s/A_v = C_2 \, K_v$, where C_2 is 4.84 for a sphere, 6 for a cube and 5.54 for a cylinder with L/D=1 and 5.86 for the present cylinder with an L/D of 2.8. This then converts Eq. 6 into Eq. 9 and this has the same form as in the European vent design guidance [Andrews and Phylaktou, 2010 and Kasmani et al., 2010b].

12th International Symposium on Hazards, Prevention and Mitigation of Industrial Explosions
Kansas City, USA - August 12-17, 2018

XII ISHPMIE
Kansas City, MO August 12–17, 2018

$$1/K_v = A_v/V^{2/3} = C_1 C_2 \ \varepsilon^{-1} \lambda \ U_L \ (E_p-1) \ P_{red}^{-0.5} \qquad (9)$$

If Eq. 9 is used for a cube and P_{red} is converted from Pa to bar then with $E_p = 8.05$ Eq. 9 becomes Eq. 10.

$$1/K_v = 0.170 \ \varepsilon^{-1}\lambda \ U_L \ P_{red}^{-0.5} \qquad (10)$$

For propane with $U_L=0.46$ m/s and taking $\varepsilon = 1$ and $\lambda = 1$ Eq. 10 becomes Eq. 11.

Table 3: *Bartknecht's (1993) values fo*r the constants *'*a*'* and n in Eq. 12.

Gas	K_G bar m/s	- n	a_{10} 10m^3	a_1 1 m^3	a Laminar Flame Theory n = -0.5	$a_{10}/a_{laminar}$ Turbulence Factor λ	$a_1/a_{laminar}$ Turbulence Factor λ
Methane	55	0.572	0.164	0.133	0.063	2.60	2.11
Propane	100	0.580	0.200	0.157	0.078	2.56	2.01
Propane Excluding 10m^3	100	0.616		0.154	0.078		
Coal Gas	140	0.590	0.212	0.171			
Hydrogen	550	0.585	0.290	0.231	0.46	0.63	0.50

$$1/K_v = 0.078 \ P_{red}^{-0.5} \qquad (11)$$

The constant in Eq. 11 is for propane and the laminar flame venting constant for other gases is given in Table 3. The form of Eq. 11 is the same as that used by Bartknecht [1993] in Eq. 12.

$$1/K_v = a \ P_{red}^{-n} \qquad (12)$$

Bartknecht's Eq. 12 is used in EN14994:2007 and the venting constant 'a' in Eq. 12 for methane, propane, coal gas and hydrogen are shown in Table 3, although these are not stated directly in EN149942007, but are in Bartnecht [1993]. In the following analysis it is assumed that the P_{red} exponent in Eq. 12 is -0.5 as for laminar flame venting theory and not the values in Table 3. Bartknecht's experimental results fit a -0.5 P_{red} exponent at low P_{red} and it is his inclusion of P_{red} in the sonic flow region that increased the exponent value. Bartknecht's constant for propane in Table 3 was 0.200. This implies a λ value of 2.56 for agreement with Eq. 10, as shown in Table 3, which gives a 6.57 factor difference in P_{red} for the same K_v. Bartknecht (1993) carried out vented explosions for propane in vessels of 1, 2, 10, 30 and 60m^3, but the value of the constant in Table 3 was for the 10 m^3 vessel as the constant was lower for all the other volumes. If the Bartknecht 10 m^3 vented data is ignored, as not agreeing with his data at four other volumes that he used, then a λ of only 2.1 is required for agreement with Eq. 10, as shown in Table 3. For methane, Bartknecht only investigated venting in 1 and 30 m^3 vessels and the constant in Eq. 11 of 0.164 was for the 30 m^3 vessel. The prediction of Eq. 10 needs a turbulence factor λ of 2.60 for agreement, which gives a 6.78 factor difference in P_{red} for the same K_v. For hydrogen Bartknecht only carried out vented explosion in the 1 m^3 vessel. Bartknecht's constant in Eq11 for hydrogen was 0.29 which is less than the laminar flame prediction of 0.46, which implies a <1 turbulence factor. A

12th International Symposium on Hazards, Prevention and Mitigation of Industrial Explosions
Kansas City, USA - August 12-17, 2018

XII ISHPMIE
Kansas City, MO August 12–17, 2018

constant in Eq. 11 of at least 1.2 would be expected from laminar flame theory. This leads to the conclusion that the Bartknecht venting constant has to be unreliable for hydrogen and needs re-evaluating in the European gas venting standard. Bartknecht [1993] correlated the mixture reactivity constant 'a' in Table 3 and Eq. 12 with his measured values of K_G in Table 2 to give Eq. 13 for $P_{stat} = 0.1$ bar.

$$1/K_v = (0.1265 \log K_G - 0.0567) P_{red}^{-0.5817} \tag{13}$$

The mixture reactivity term in Eq. 13 is that used in the European gas venting standard EN14994:2007. However, Table 1 shows that Bartknecht's data is unreliable for K_G as the difference between methane and propane, with propane being 82% more reactive than methane, is too great, relative to the 7% difference in U_L. In addition the evaluation of 'a' in Eq.12 in different sized vented explosion vessels is undesirable as the different vessels give different values of 'a' for propane, so comparison of mixture reactivity using different volumes is undesirable. Thus, the impact of mixture reactivity on P_{red} in gas venting is unreliable in EN14994:2007 and Eq. 13 needs revision. The present work presents data for methane, propane, ethylene and hydrogen, all at the maximum reactivity concentrations.

There are several problems with the above laminar flame theory. The theory assumes that all the unburned mixture is expelled from the vessel before the flame emerges from the vent and this does not occur in reality [Cooper et al., 1986; Cates and Samuels, 1991]. If this was a valid assumption then P_{fv} and pressure at which the flame touched the wall and had a maximum flame area, P_{mfa}, would occur at the same time and be the same overpressure, it will be shown in this work that this does not occur and that in most cases P_{fv} occurs before P_{mfa} and that P_{mfa} is very rarely the peak overpressure. Cates and Samuels [1991] have shown from experimental results that the flame surface area at the peak overpressure was twice the cross-sectional area of the vessel for low K_v. For a cubic vessel this is equivalent to 1/6 of A_s and for a cylinder, with an L/D of 1, 1/3 of A_s and for an L/D of 3, 1/7 of A_3. Thus the classic laminar flame theory should over predict measured venting overpressures by a factor of 3-7 depending on the vessel L/D. The results show that Eq. 13 is incompatible with the data, which follows the trends with U_L in Eq. 10 as used in NFPA68.

This comparison for methane is shown in Fig. 2 which shows that the laminar flame theory and NFPA68 [2013] venting equations , Eqs. 9 and 10, are similar. However, both predict higher over pressures than those measured in the 10L vented explosion results and other vented explosions. The reason for the over prediction was the assumption in the laminar flame theory that P_{red} occurred at the maximum flame area upstream of the vent, which was assumed to be the surface area of the vessel walls, A_s. The results show that this is not the case and the difference is the ratio of the actual flame area to A_s. Also Fig. 2 shows that there are results in the literature that are also below the laminar flame venting theory prediction and other results with higher values. The experimental results of Bartknecht [1993], on which the EU vent design standard is based are significantly above other literature measurements and significantly above the laminar flame theory predictions. It was shown above that a turbulence factor of 2.56 is required for agreement with laminar flame venting. One possible source of this turbulence is the interaction of the vented jet with the ground, as all Bartknecht's [1993] vessels had the bottom of the vessel on the ground.

3. Experimental Methods

The small 10L vented explosion vessel with a diameter of 162mm and an L/D of 2.8 is shown in Figure 2 and Figure 1 shows the P_{red} results for this vessel with end wall ignition, where they are compared with other vented vessel P_{red} from the literature. Figure 1 is for free venting or very low P_{stat} venting. It shows that the 10L vented vessel has P_{red} values close to the

laminar flame venting predictions. The vent outlet was connected to the dump vessel using a 0.5m diameter pipe connection, which had no influence on P_{red}.
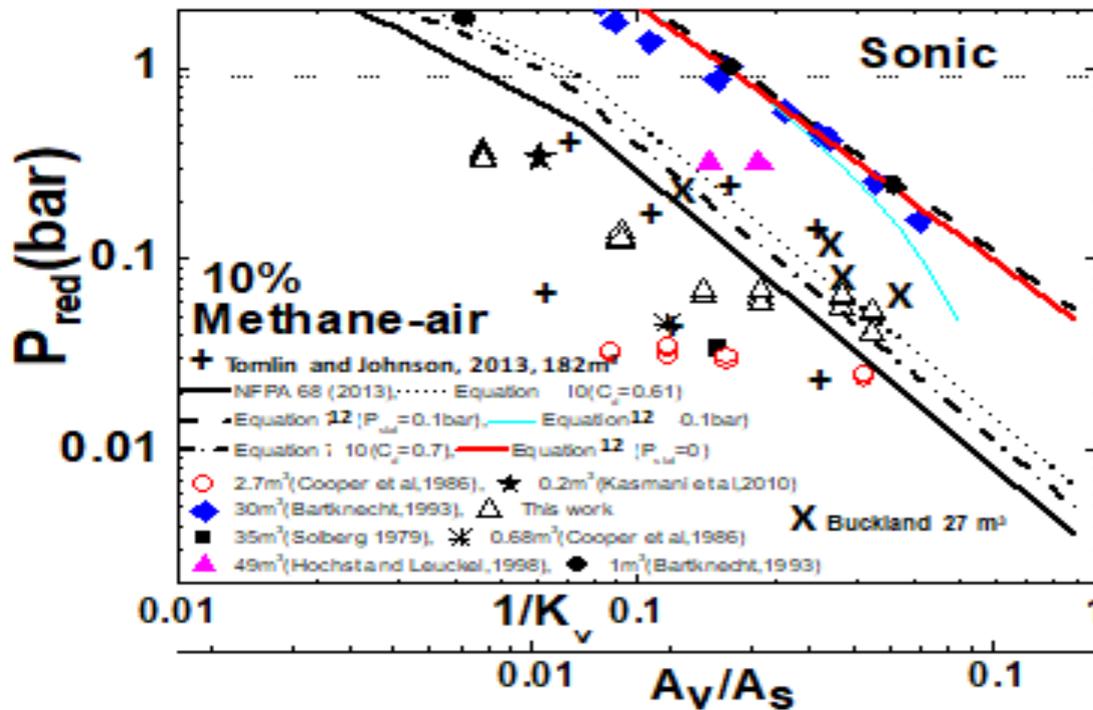
Figure 2: Comparison of the 10L vented explosion results with literature values of P_{red} for 10% methane-air vented explosions as a function of $1/K_v$ and A_v/A_s for a cubic volume, together with comparison with US and EU vented guidance and laminar flame venting theory.
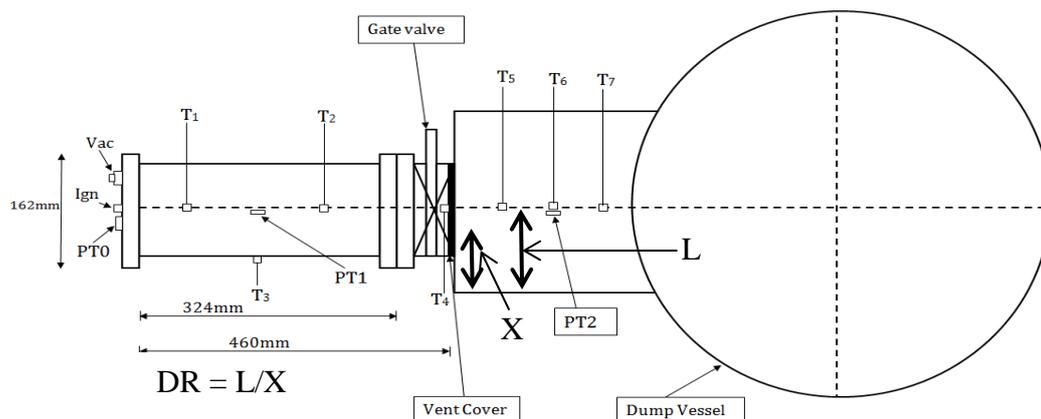
Figure 3: 10L small vented vessel with a large vessel surrounding the vent outlet

The explosion vessel was fitted with thermocouples T_1 and T_2 at 0.5D and 1.5D from the end flange as well as T_4 in at the vent outlet plane. All these thermocouples were on the vessel centreline, which enabled the flame speeds to be determined as well as the time the flame

12th International Symposium on Hazards, Prevention and Mitigation of Industrial Explosions
Kansas City, USA - August 12-17, 2018

XII ISHPMIE
Kansas City, MO August 12–17, 2018

arrived at the vent, T_4. There were also thermocouples mounted downstream of the vent so that the external flame speed could be determined (T_5, T_6 and T_7). This array of thermocouples enabled the flame speed as a function of distance from the spark to be determined. In addition there was a thermocouple mounted close to the wall on the centre of the vessel, T_3. This was used to determine the time the flame reached the wall and to show whether combustion inside the vessel was completed before the flame left the vent, as assumed in the laminar flame theory. If T_3 was well after the flame left the vent, as it was for methane and propane explosions (Fakandu et al., 2011, 2016b), then the combustion of this unburned mixture might control the peak overpressure.

Peizo resistive pressure transducers were mounted flush with the wall in the end flange (P0) near the spark plug and on the vessel wall half way down the length (P1) as shown in Fig. 3. There was no difference in these two pressure transducers for methane, propane and ethylene explosions, but major differences in hydrogen flame explosions (Fakandu et al., 2012).

The ignition position was at the end flange, because this is the worst case P_{red} for the L/D 2.8 configuration of the tests. Fakandu et al. [2014] have compared end and central ignition vented explosions and shown that end ignition has the highest P_{red}. They also reviewed the literature on this and showed that most experimental data supported end wall ignition, opposite the vent, as the worst case ignition location in vented explosions. However, most of the experimental data in Fig. 2 was for central ignition.

4 The Influence of Gas Reactivity on the Pressure as a Function of Time

4.1. Influence of gas reactivity at K_v=4.3 (50% vent blockage) for stoichiometric gas/air mixtures where the external explosion, P_{ext}, was the larger overpressure.

The pressure time records for free vented explosions for K_v=4.3 with end ignition for the maximum reactivity mixture for propane and ethylene-air mixtures are shown in Fig. 4a and b respectively. The time of flame arrival at the thermocouple locations are also shown. Fig. 4 shows that for both gases the external explosion after the flame has left the vent was the highest overpressure, P_{ext}. The two pressure peaks for the flow through the vent orifice plate flow pressure loss, P_{fv}, and P_{ext} are clearly separated with a significant difference in their magnitude. The time of arrival at the wall thermocouple is also shown, which is the time of maximum flame area and this does not control the peak overpressure, as assumed in the laminar flame venting theory. Comparison of Fig. 4 a and b shows that the more reactive ethylene-air mixture has a much higher P_{ext}, but the characteristics of the explosions are very similar.

The pressure time record for the maximum reactivity for methane-air explosions is shown in Fig. 5 together with the stoichiometric explosion records for propane, ethylene and hydrogen. For 10% methane-air P_{ext} is the highest overpressure and is significantly higher than P_{fv}. For stoichiometric mixtures in Fig. 5 the peak overpressure was P_{ext} but the P_{fv} was of a similar magnitude for propane and ethylene. However, for stoichiometric hydrogen explosions the large pressure rise due to the flow through the vent was the dominant overpressure. The pressure rise was very large and would give sonic flow at the vent. The peak overpressures and whether it was P_{ext} or P_{fv} is summarized in Table 4 for stoichiometric (Ø=1) and the most reactive mixtures (MR).

The maximum reactivity 40% hydrogen air vented explosion pressure time records are shown in Fig. 6 for two repeat explosions and for the end wall (P0) and side wall (P1) pressure transducers. The pressures at P1 were higher than P0 and this was due to dynamic flame events. The first vented explosion showed that the P_{fv} was the highest overpressure due to the

sonic flow induced through the vent. However, the repeat explosion showed lower overpressures with P_{ext} as the highest overpressure. The reason for this difference is not known, but the first results were the worst case and these have been shown in Table 4.

Table 5: Summary of the peak overpressures (bar) for methane, propane, ethylene and hydrogen for free venting in a 10L cylindrical vessel with L/D=2.8 for end ignition.

K_v	4.3	4.3	4.3	4.3	21.4	21.4
	P_{fv}	P_{ext}	P_{fv}	P_{ext}	P_{fv}	P_{ext}
Mixture	Ø=1	Ø=1	MR	MR	Ø=1	Ø=1
Methane			0.023	0.030	0.18	0.13
Propane	0.024	0.025	0.03	0.053	0.45	0.38
Ethylene	0.072	0.080	0.12	0.18	1.20	1.05
Hydrogen	3.0	0.45	4.0	0.5	5.3	2.0

(a)   (b)
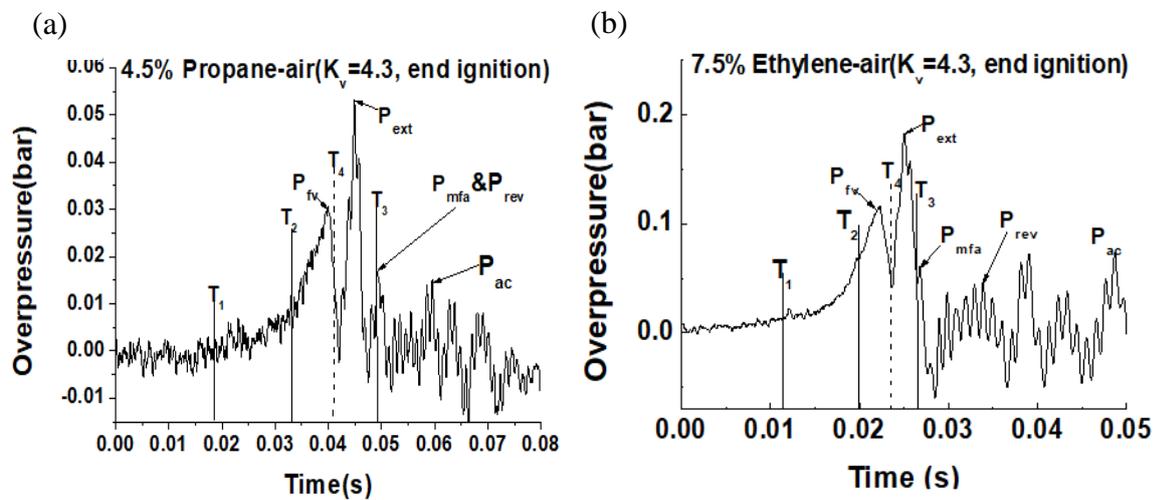
Figure 4: Pressure time records for free vented explosions for the maximum reactivity mixtures for (a)Propane and (b) ethylene for $K_v = 4.3$ with end ignition opposite the vent.
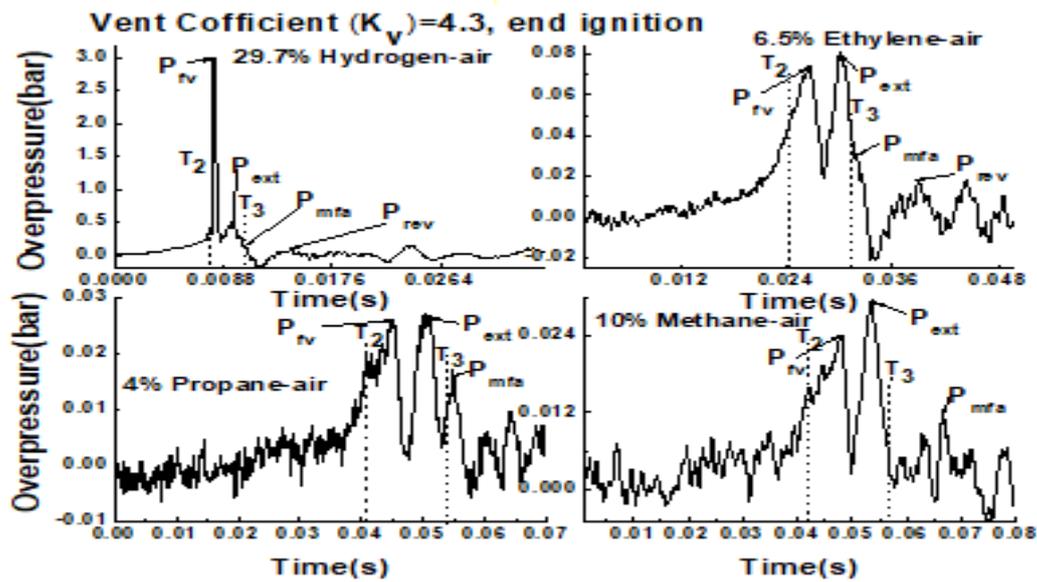
Figure 5: Pressure-time records for hydrogen, ethylene and propane with stoichiometric mixtures and methane-air at the maximum reactivity mixture for Kv=4.3
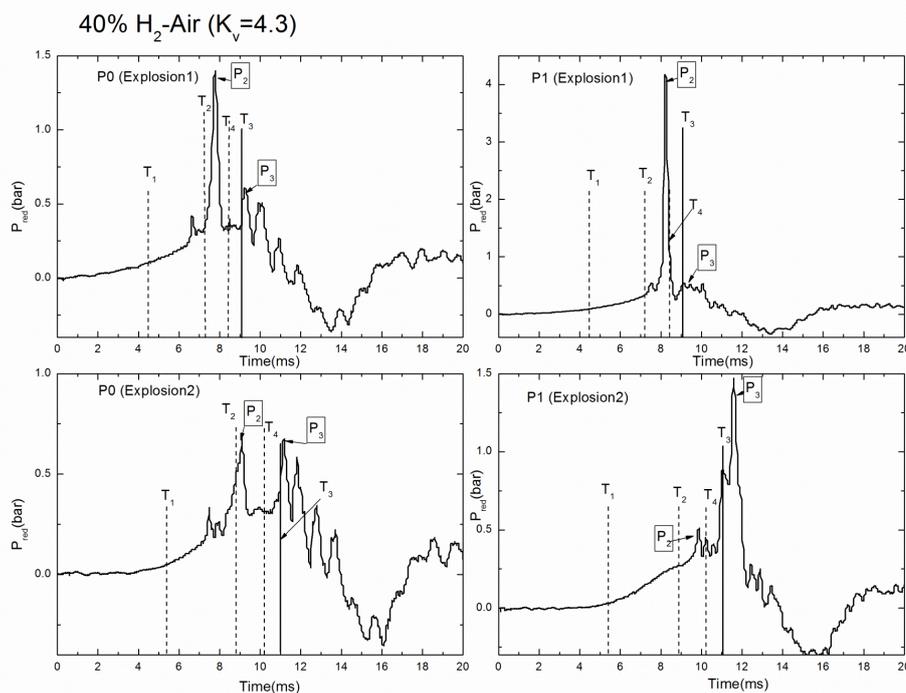
Figure 6: Pressure records for two repeat vented explosions for 40% hydrogen-air with $K_v = 4.3$ (blockage ratio 50%), comparison of the P0 (left) and P1 (right) pressure transducers in Fig. 3

The assumption in the simple laminar flame venting theory that the flame had an area of A_s at the time of the peak overpressure is shown in these results to not be valid for stoichiometric and maximum reactivity for all the gas reactivities. If it was valid the time of arrival at T_3 would be the same as the time of occurrence of peak overpressure. This means that the measured overpressure should be less than that predicted, as was found and shown in Fig. 1. It will be shown later that the flame speed towards the vent was much greater than for a

spherical laminar flame speed, so that the assumption in the laminar flame venting theory of spherical laminar flame propagation prior to the vent was also not valid.

The problem with developing a prediction procedure for the external explosion, P_{ext}, is that this needs to know the flow rate of unburned gases out of the vent, in order to compute the vent induced turbulence. This computation is the same as that involved in the simple laminar flame theory here. Also, this computation requires the area of the flame to be known in order to calculate the mass combustion rate and hence the mass flow of unburned gas through the vent. Thus the two approaches to modelling the overpressures, P_{fv} and P_{ext}, are interlinked. In the laminar flame venting theory the flame area at the maximum overpressure was taken as the surface area of the vessel, A_s. Cates and Samuels (1991) stated that their video records of vented explosions supported a flame area at the maximum overpressure that was twice the cross sectional area of the vessel, which for a cubic vessel is 1/3 of A_s. Bauwens (2010) presented empirical expressions for the maximum flame area for venting with rear wall ignition and central ignition. Fakandu et al. (2016a) have shown that the Taylor's equation gives a reasonable prediction of P_{ext} based on the measure flame speed downstream of the vent.

The stoichiometric hydrogen-air vented explosion results in Figs. 5 and 6 for K_v=4.3 were significantly different for those of the other less reactive gases. The overpressure rose to 0.25 bar just as the flame passed T_2, but then there was a very large pressure increase to 3.0 bar just as the flame passed through the vent, which indicates sonic flow at the vent (sonic flow for air occurs at a pressure ratio of 1.9 or an overpressure of 0.9 bar). The second peak pressure P_{ext} at 0.5 bar was due to a very fast external explosion [Harris and Wickens, 1989]. Once the vent flow was sonic the mass flow of unburned gas through the vent was a linear function of the upstream pressure. Thus, as the upstream mass burning rate continues to increase the pressure due to sonic flow through the vent increases linearly with the mass burning rate. It may be that hydrogen is a special case as none of the other gases are sufficiently reactive to generate sonic flow at the vent at a K_v of 4.3. In Bartknecht's work in Fig. 1, sonic flow for methane in a 30 m^3 vessel occurred at a K_v of 5.6. Fig. 1 shows that for methane no other workers in vented vessels record sonic flow overpressures occurring for methane at these K_v.

The external explosion for stoichiometric hydrogen in Figs. 5 and 6 was significant at about 0.4 bar overpressure, but this was well below the large peak pressure caused by sonic flow at the vent. There was a significant period after the flame exited the vent until T_3 recorded flame arrival at the wall. This was surprising as the radial spread of hydrogen into the wall region was expected to be fast, but the results in Figs. 5 and 6 show a very similar time from the flame arrival at T_2 to its arrival at T_3 at about 0.02 – 0.025s irrespective of the reactivity of the mixture. For a maximum radial flame movement of 81mm, this implies an average radial flame speed of about 4 m/s irrespective of the reactivity. This is close to the burning velocity for stoichiometric hydrogen air, but much higher than the burning velocity for the other gases. This indicates that the flame burned into the trapped unburned hydrogen-air mixture at the laminar burning velocity with the production of burned gas vented out of the vent and not trapped, so that it increased the flame speed. Thus the venting of burnt gases stops the burnt gas expansion increasing the flame speed and the flame propagation slows to the burning velocity as it burns the remaining mixture trapped upstream of the vent.

4.2 Influence of Gas Reactivity at K_v=21.7 (90% vent orifice blockage)

Fig. 3 shows that the smallest vent size investigated in the work of Bartknecht [1993] was a $1/K_v$ of 0.03, but most of the data was limited to $1/K_v$ of 0.05 or K_v of about 20. Consequently, in the present work this very low vent area or very high K_v effect was

12th International Symposium on Hazards, Prevention and Mitigation of Industrial Explosions
Kansas City, USA - August 12-17, 2018

XII ISHPMIE
Kansas City, MO August 12–17, 2018

investigated for a K_v of 21.7, which corresponds to a vent with a 90% blockage of the cross sectional area of the cylindrical explosion vessel. The pressure time records for stoichiometric methane, propane, ethylene and hydrogen are shown in Fig. 7. As expected, all the overpressures were much higher than for K_v=4.3 in Fig. 5. This work was the first to be completed in this research and thermocouples T_3 and T_4 were not fitted. However, all the results show that the peak overpressures occurred soon after the flame passed thermocouple T_2. The pressure peak P_{fv} was always the dominant peak for K_v=21.7, in contrast to K_v=4.3 where P_{ext} was the dominant peak for methane, propane and ethylene. For propane Fig. 7 shows evidence of a second pressure rise event that creates a 'shoulder' in the pressure fall from the main P_{fv} peak at a time of 0.055s. This indicates that for propane the P_{fv} and P_{ext} events were merged into one overall pressure peak. The reason for the dominance of P_{fv} at high K_v is that displacement of unburned gas by the advancing expanding flame upstream of the vent is similar at the two K_vs, as shown below, but the pressure loss of this flow through a smaller vent is much higher and is the dominant source of the overpressure, as assumed in the simple laminar flame theory.

For methane and propane Fig. 7 shows that the peak overpressure was in the subsonic vent flow regime. However, for ethylene and hydrogen the peak overpressure was >0.9 bar and hence sonic flow occurred at the vent. This occurred soon after the flame passed T_2. The laminar flame venting theory in Eq. 9, which assumes incompressible flow at the vent, can be
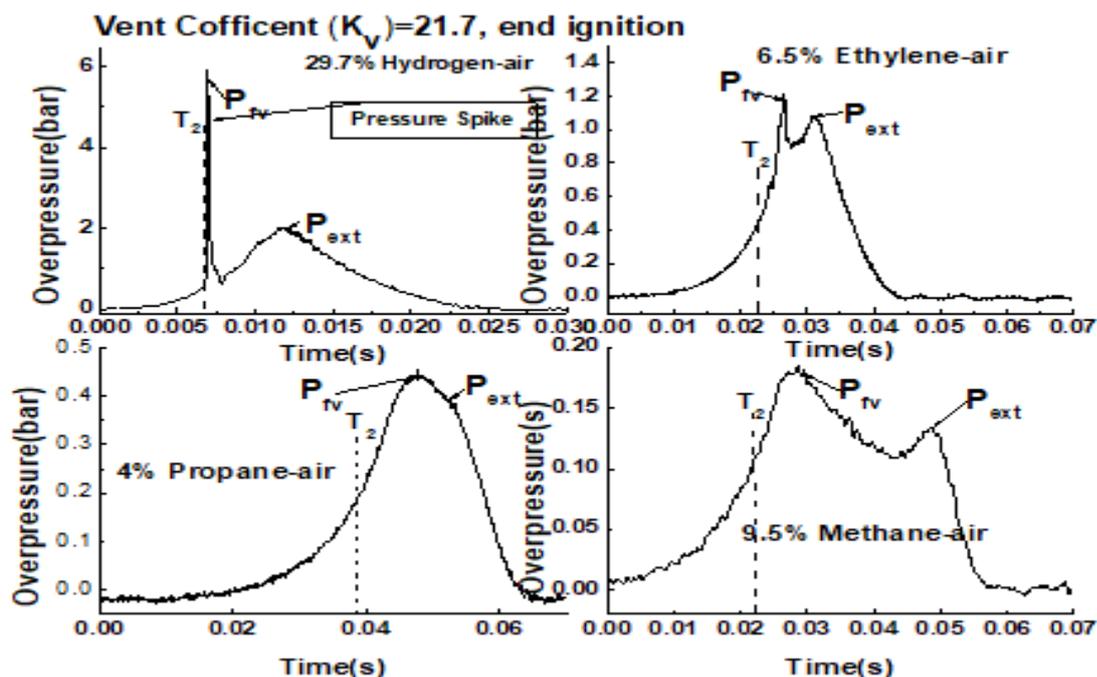
Figure 7: Pressure-time and flame time of arrival for different fuels for stoichiometric mixtures with K_v=21.7
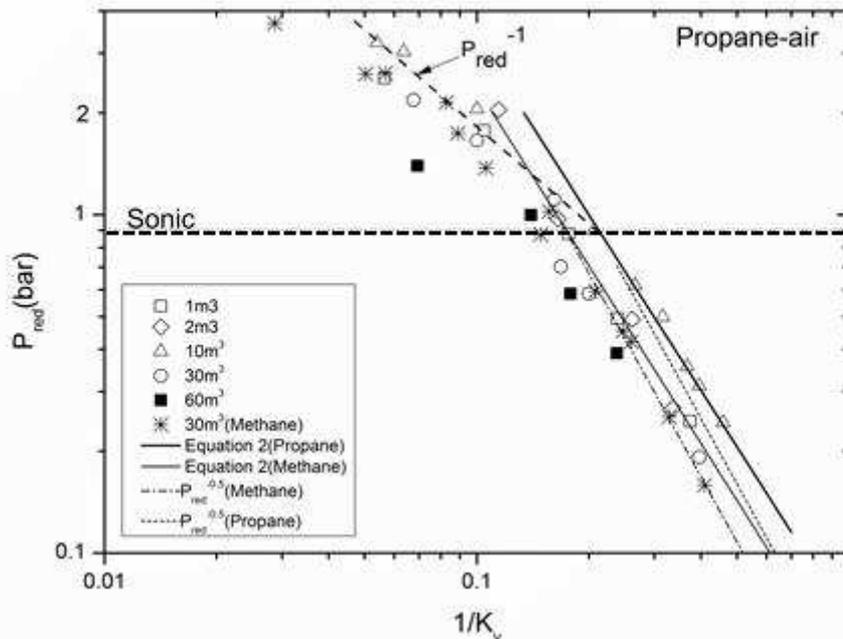
Figure 8: Bartknecht's(1993) vented explosion experimental data for propane (1 – 60 m³) and methane (30 m³)

converted into a sonic vent flow version by replacing the orifice plate flow equation with the orifice sonic flow equation (Fakandu et al., 2016b) and then Eqs. 13 and 14 result.

$$U_L(E_p - 1)\rho_u A_s = 0.0404\, P_o/T_o^{0.5} A_v = 0.00233\, P_o A_v \text{ for } T_o = 300K \quad (13)$$

$$A_v/A_s = U_L(E_p - 1)\rho_u / 0.00233\, P_o \quad (14)$$

where $P_o = P_a + P_{red}$

For sonic flow at the vent the overpressure due to the mass flow of unburned gas scales linearly with the mass flow rate and this dependence has been plotted for the laminar flame theory prediction in Fig. 2 for $P_0/P_a > 1.9$ where critical flow occurs for air, which is a P_{red} of >0.9 bar. Fig. 8 shows the experimental venting data of Bartknecht (1993) and 50% of this data was in the sonic venting region. Fig. 8 shows that the linear dependence on pressure of Eq. 14 gives a good correlation of the data for Bartknecht for the 10m³ vessel for $P_{red} > 0.9$ bar. Comparison of Figs. 4-7 for hydrogen shows that for K_v between 4.3 and 21.7 the vent flow will be sonic for hydrogen, but for ethylene will only be sonic at the highest K_v. Fig. 8 also shows that the incompressible venting correlation of the data should not be extended to P_{red} of 2 bar, as in the range of validity of the Bartknecht (1993) and En14994:2007.

For ethylene and hydrogen there was a significant overpressure P_{ext} due to the external explosion, which was lower than the P_{fv} overpressure due to sonic flow of unburned gas through the vent. This was because at a K_v of 21.7 the jet velocity through the vent was very high and this created high turbulence in the downstream unburned gas flow as well as a high orifice vent flow pressure loss. For ethylene and hydrogen this second overpressure was above 1 bar and indicates a very high flame speed in the external explosion. The 2 bar P_{ext} overpressure for hydrogen air in Fig. 7 would need an external flame speed of 450 m/s to account for this and the 1.1 bar P_{ext} for ethylene-air would require 320m/s flame speed [Harris and Wickens, 1989]. Downstream flame speeds were not determined in the present work, but

12th International Symposium on Hazards, Prevention and Mitigation of Industrial Explosions
Kansas City, USA - August 12-17, 2018

XII ISHPMIE
Kansas City, MO August 12–17, 2018

the upstream flame speed was and these are presented below. The acceleration by the turbulence created by the vent, as an obstacle to the explosion with 90% blockage, is capable of accelerating the fast flame upstream of the vent into speeds 10 times faster downstream [Phylaktou and Andrews, 1991].

5. Influence of Gas Reactivity on Flame Speeds Upstream of the Vent

The time of arrival at the two bare bead thermocouples on the vessel centreline was used to determine two flame speeds: the initial flame speed for the time of the flame travel from the spark to the first thermocouple, T_1, and the later flame speed determined as the time of travel from T_1 to T_2. The two flames speeds are shown as a function of the mixture reactivity K_G and U_L, as well as the laminar spherical flame speed U_L E_p in Figures 9a-f for K_v=4.3 and 21.7. These results show that the three methods of characterising the mixture reactivity resulted in flame speeds that were reasonably linearly related.

Figs. 9a and 9b show for K_V=4.3 the flame speeds as a function of mixture reactivity in terms of K_G and U_L respectively and this shows a more linear relationship with U_L, mainly due to the large differences in K_G for methane and propane, which is not proportional to the U_L differences for these gases. The initial flame speed was close to the spherical flame speed as shown in Fig. 9c. The final flame speed was much higher than the spherical flame speed, which is the main reason why end ignition gives higher overpressures than for central ignition (Kasmani et al., 2010b). The linear relationship between the two flame speeds and mixture reactivity, U_L, shows a constant ratio between the later and initial flame speeds of about 2.5 for all mixture reactivities, as shown in Fig. 9b and c.

For the high K_V of 21.7 the results in Fig. 9 d-f were quite similar to those for K_v=4.3, with a near linear relationship between the two flame speeds and the mixture reactivity in terms of U_L and the spherical laminar flame speed $U_L E_p$. The initial flame speed was similar to that for a spherical flame, as shown in Fig. 9f, which was also found in Fig. 9c for K_v=4.3. This was expected as the flame on the far wall was too far from the vent to be influenced by the vent open area. However, the later flame speed was also similar to that for methane/air at K_v=4.3,

12th International Symposium on Hazards, Prevention and Mitigation of Industrial Explosions
Kansas City, USA - August 12-17, 2018

XII ISHPMIE
Kansas City, MO August 12–17, 2018
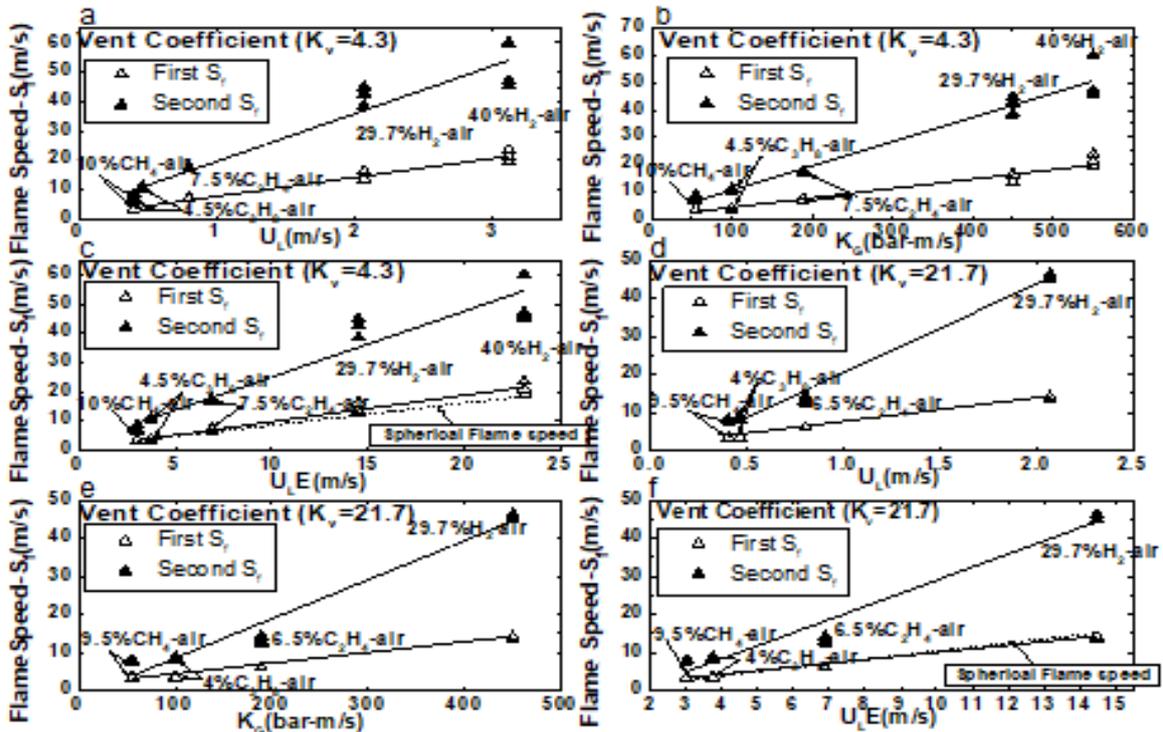
Figure 9: Initial and later flame speeds as a function of mixture reactivity for K_v=4.3 (a) – (c) and K_v=21.7 (d)-(f).

but was lower for propane and ethylene and similar for hydrogen to the later flame speeds for K_v=4.3.

These flame speed results show a flame acceleration ratio of the later to the initial flame speeds of about 3 for methane and hydrogen but about 2.3 for propane and ethylene. This ratio for a K_v of 4.3 was about 2.5 for all reactivities. However, the present data indicates that there is no major influence of K_v on the ratio of later to initial flame speeds and a mean acceleration factor of about 2.5 would be reasonable to assume from these measurements for all mixture reactivities.
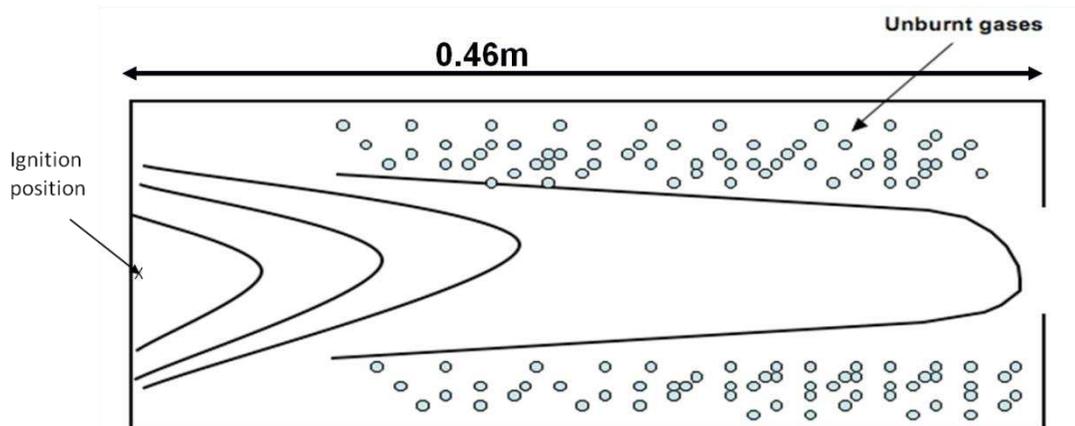
Figure 10: Flame Movement Pattern in 0.46m long cylindrical vessel

12th International Symposium on Hazards, Prevention and Mitigation of Industrial Explosions
Kansas City, USA - August 12-17, 2018

XII ISHPMIE
Kansas City, MO August 12–17, 2018

There are three mechanisms that can cause the flame to accelerate towards the vent:

a. Expansion of the flame by the burned gases only in the direction of the vent flow and not spherically, which is in agreement with earlier work by Phylaktou et al. (1990) as shown in the sketch in Figure 10.

b. The 0.46m flame travel distance is sufficient for cellular flames to develop, as for many flames this starts at ~0.1m (Harris and Wickens, 1989). Using the correlation of Cates and Samuels (1991) for this effect would lead to an acceleration distance beyond the critical size of 0.1m for cellular flame development of 0.36m and a cellular flame self-acceleration factor of 1.2 for propane.

c. The vent outflow velocity, which increases as K_v increases, drags the flame towards the vent as shown schematically in Fig. 10.

A constant factor of about 2.5 for all the gas reactivities would not be expected if cellular flames were the cause of the acceleration, the acceleration for hydrogen and propane should be greater than methane (Bradley, 1997). Also the acceleration factor for propane was 1.2 using the Cates and Samuels (1991) correlation and this is too small to account for the observed flame acceleration. As the vent flow velocity increases with K_v and the flame speed upstream of the vent does not, then the suction effect of the vent is unlikely to be the cause of the increased flame speeds. Thus, it is concluded that the increased downstream flame speeds were due to the preferential expansion of the flame in the axial direction of the vent. Andrews and Phylaktou (1990) demonstrated this for large L/D vessels with no venting. They showed that at an L/D of 3 the axial flame speed was about 3 times the laminar spherical value, close to that found in this work.

6. P_{red} as a Function of Mixture Reactivity

The influence of the mixture reactivity K_G on P_{red} is shown as a function of K_G in Fig. 11 for $K_v = 4.3$. The results for P_{fv} and P_{ext} in Figs. 4-7 have been included as well. All tests were repeated three times and the individual data points are included in Fig. 11. The values of K_G were those in Table 1 from Bartknecht [1993]. No value for ethylene was determined by Bartknecht and this was estimated as a linear relationship with the laminar burning velocity using propane K_G=100 bar m/s and laminar burning velocities of 0.46 for propane and 0.80 for ethylene, this gave a K_G for ethylene of 174 bar m/s. The measured values for ethylene in a 1 m^3 vessel are shown in Fig. 1 to be a K_G of 215 bar m/s and a U_L of 94 cm/s. These are higher than the above estimated values based on Bartknecht's measurements. The stoichiometric and maximum reactivity mixtures for hydrogen have also been included in Fig. 11 and the same method as above for ethylene was used to determine the K_G for stoichiometric hydrogen-air, using the burning velocity measurements of Andrews and Bradley [1973] for hydrogen-air as a function of equivalence ratio. The experimental results show a very strong influence of mixture reactivity at K_v=4.3 with sonic venting for both the hydrogen explosions. An improved correlation with K_G could be achieved if the Bartknecht values for K_G were replaced with those measured in the 1 m^3 explosion vessel.

The overpressures P_{fv} and P_{ext} are shown separately in Fig. 11 and these have slightly higher P_{ext} for methane, propane and ethylene and much higher P_{fv} for hydrogen. This was due to the higher velocities through the vent as the reactivity increased, which created higher vent orifice flow pressure loss and hence higher P_{fv}. The Bartknecht (1993) vent design equation prediction of the influence of reactivity in Eq. 12 and 13 is shown in Fig. 11 for comparison with the experimental data. The laminar flame theory of Eq. 6 is shown for comparison with the P_{fv} results in Fig. 11. The theory was corrected for sonic flow at the vent using a linear

12th International Symposium on Hazards, Prevention and Mitigation of Industrial Explosions
Kansas City, USA - August 12-17, 2018

XII ISHPMIE
Kansas City, MO August 12–17, 2018
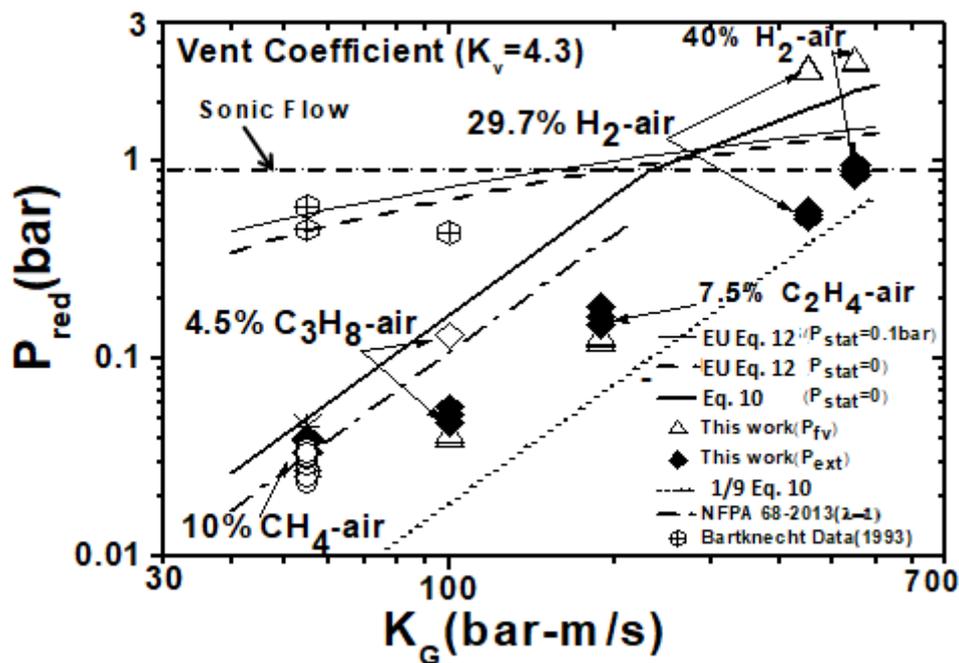
Figure 11: P_{red} as a Function of K_G with Comparison with Eqs. 7, 10 and 12.

dependence of vent mass flow on the overpressure, as shown in Eq. 18, instead of the square root dependence for incompressible flow in Eq. 6. Fig. 11 also compares the prediction of the reactivity effect from Eq. 7 from NFPA 68 [2013] for $\lambda = 1$, with A_s converted to a function of $V^{2/3}$ using a cubic vessel relationship.

Fig. 11 shows that the laminar flame venting theories of Eq. 6 gives much better agreement with the experimental data than that of the Bartknecht vent design Eqs. 12 and 13, which grossly over predicts P_{red} at low K_G and under predicts at high K_G. Fig.11 shows the square root relationship in Eq. 10 for the dependence of P_{fv} on K_G is not demonstrated in the experimental results for methane and propane. This is most likely due to the measurement of K_G for methane being too low and their relative values being inconsistent with the more common reactivity parameter U_L. Fig. 11 shows that the theories in Eqs. 10 over predict the present experimental P_{fv} results for methane, propane and ethylene, but only by a small margin for methane. This was due to the assumption that the flame area was A_s at the time the flame exited the vent. The time of flame arrival at the wall thermocouple T_3, which was shown above to be well after the flame had left the vent, shows that this assumption is not valid. However, the trend for the influence of K_G is reasonably well predicted.

For hydrogen the theory under predicts the measured P_{fv} results as shown in Fig. 11. This suggests that there was an additional acceleration mechanism for hydrogen, possible self-acceleration, due to the development of cellular flames. Comparison with Eq. 12 for Bartknecht's results is also shown in Fig. 11 which indicates that this does not predict the influence of mixture reactivity adequately. There was a gross over prediction of the low K_G results and a significant under prediction of the hydrogen results. Correcting Eq. 12 for the 0.1 bar static burst pressure used does not account for the over prediction that occurs, as shown in Fig. 1. The under prediction of the hydrogen results using Eq. 12, which is adopted in the EU vent design guidance, is of concern and more work on hydrogen explosion venting is required and the vent design guidance for hydrogen needs to be revised. It is possible that in Bartknecht's results the P_{fv} pressure rise was ignored as too short a pressure pulse for the

12th International Symposium on Hazards, Prevention and Mitigation of Industrial Explosions
Kansas City, USA - August 12-17, 2018

XII ISHPMIE
Kansas City, MO August 12–17, 2018
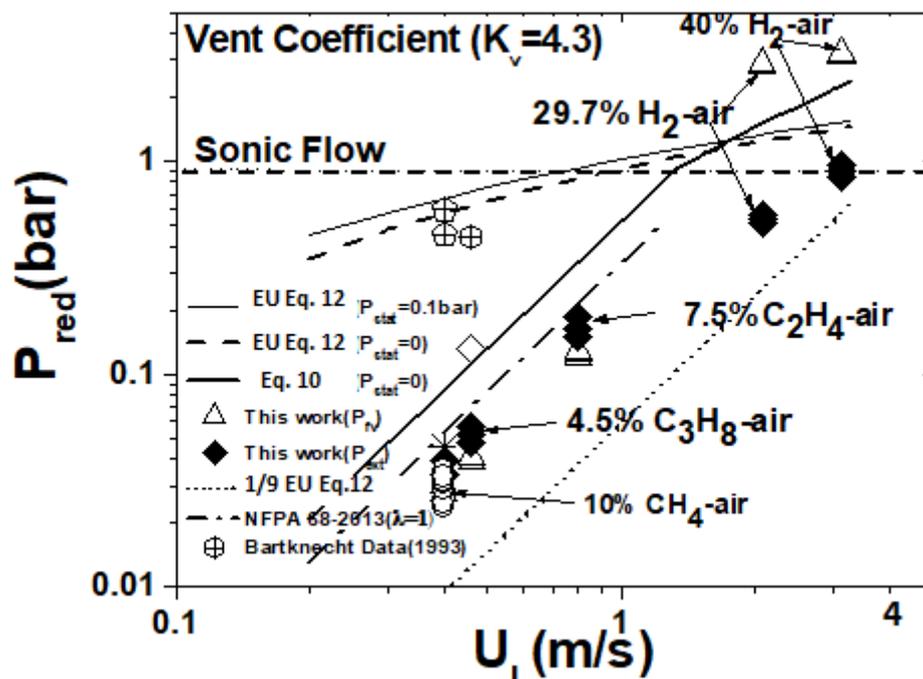
Figure 12: P_{red} as a Function of U_L for K_v=4.3 with Comparison with Eqs. 6 and 9

vessel to respond to and that the peak overpressure was taken as the external flame pressure P_{ext}, which Eq. 12 does predict reasonably well for hydrogen. However, the pressure records for Bartknecht's vented explosions have not been published so this cannot be verified.

Fig. 12 shows the same data as in Fig. 11 for K_v=4.3 plotted as a function of the laminar burning velocity U_L, which is the more usual reactivity parameter. This shows much better agreement of the laminar burning velocity data with the laminar flame theory of Eq. 6 than is shown in Fig. 11 using K_G as the reactivity parameter. However, the magnitude of the present results are over predicted by the present laminar flame theory with $C_d = 0.61$, but are only just below the predictions of NFPA 68 [2013] where a C_d of 0.7 is used. The over prediction of the measured overpressures was because the actual flame area at the peak overpressure was not the assumed area of A_s in the theory. The flame area assumption of Cates and Samuels [1991] that the flame area was twice the cross sectional area of the vessel, would for a cubic vessel give a flame area one third of the surface area of the vessel and hence an overpressure 1/9 of that assuming the flame area was A_s would result. However, Fig. 12 shows that this gives a significant under prediction of the present results. The square root relationship between P_{fv} and U_L from the theory in Eq. 6 is supported by the experimental data for methane, propane and ethylene. This is because K_G values in Table 3 for propane and methane and hydrogen do not scale with the U_L values, which have a better experimental data base than does the K_G values of Bartknecht. The Bartknecht vent design Eq. 12 may be converted into a U_L equivalent using Eq, 2 and this has been plotted in Fig. 12. This still over predicts P_{red} for low reactivity mixtures and under predicts for hydrogen.

The P_{fv} and P_{ext} overpressures in Table 5 for $K_v = 21.7$ are shown as a function of K_G in Fig. 13. At this high K_v the experimental results show that P_{fv} was the dominant overpressure for all gas reactivities. The P_{fv} peak pressures correlate with $P_{fv}^{-0.5}$ in the subsonic vent flow regime as expected by the theory. The ethylene P_{fv} results also lie on the expected line in the sonic flow regime. The hydrogen P_{fv} results are above the expected result based on extrapolation from the lower K_G experiments. It is considered that the explanation may lie in

12th International Symposium on Hazards, Prevention and Mitigation of Industrial Explosions
Kansas City, USA - August 12-17, 2018

XII ISHPMIE
Kansas City, MO August 12–17, 2018
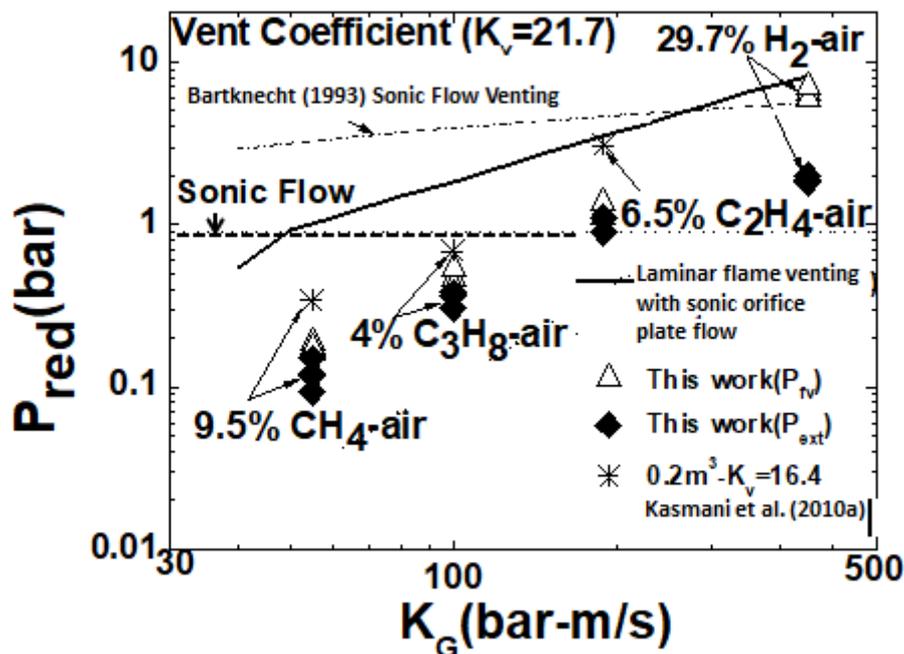
Figure 13: P_{red} as a Function of K_G for $K_v = 21.7$ (90% blockage) with Comparison with Eqs. 2 and 5

self-acceleration of hydrogen flames in this small vented explosion vessel, but no significant self-acceleration for the other gases.

Fig. 13 also compares the present results with Bartknecht's experimental results in Fig. 8 for the sonic flow regime and the laminar flame venting theory in Eq. 9. Eq. 12 and 13 predict that the vent overpressure will be in the sonic flow regime for all values of K_G for K_v of 21.4 and this is why Eq. 12 cannot be used directly as it is not valid for $P_{red} > 2$ bar and is not really valid for $P_{red} > 0.9$ bar, as Eq. 12 is essentially an incompressible vent flow equation. However, Fig. 8 shows that all Bartknecht's experimental results for $1/K_v = 0.05$ were for $P_{red} > 0.9$ bar and hence all venting is predicted to be sonic based on these experimental results for propane and methane. The sonic venting line, Eq. 14, in Fig. 13 has been taken from Fig. 8 and anchored on the propane-air data for the $10m^3$ vessel. The K_G trend has then been assumed to be the same as in Eq. 13. This methodology does enable the hydrogen overpressures to be more closely predicted than direct use of Eq. 13 would give.

Fig. 13 shows that the laminar flame theory in its sonic orifice flow version, Eq. 14, over predicts the measured results substantially and predicts sonic flow at conditions that the experiments showed were well away from sonic vent flow. Again this shows that the assumption in the theory that the flame area at the point of maximum overpressure was A_s cannot be correct. At $K_v = 21.7$ the error is much greater than at $K_v = 4.3$, as shown by comparing Figs. 16 and 11. These results show that although Eq. 6 or 10 give safe overpressure predictions, there are still venting flame shape effects that are not taken into account in the theory. However, the theory does have excellent agreement with vented explosion data in some large scale explosions as shown in Fig. 2.

The overpressure results in Figs. 11 and 13 are summarised in Table 6 and compared with the expected gas mixture reactivity effect normalised to that of methane/air. If the relationship between overpressure and U_L was that in Bartknecht's (1993) results as in Eq. 12 and 13 then

Table 6 shows that the reactivity effect is grossly under predicted for propane and grossly over predicted for hydrogen. However, the hydrogen overpressure is in the sonic regime and the vent flow rate is linear with overpressure, which would result in a linear dependence of the overpressure on U_L and the results in Table 6 for sonic flow are in approximate agreement with this for hydrogen. However, these results at high K_v indicate a more complex influence of mixture reactivity than in the simple laminar flame venting theory. Table 5 shows good agreement between the measured normalised overpressures and the normalised values of the deflagration index K_G. If the flow was incompressible then the relationship should be with K_G^2 and linear with K_G only for sonic flow. Also, the unusual high increase in reactivity between methane and propane in the K_G factor requires further validation as there is no kinetic reason for this. Table 6 also shows that the present results show no agreement with the reactivity trends in the Bartknecht vent design Eq. 12 with the constants for 'a' from Table 3.
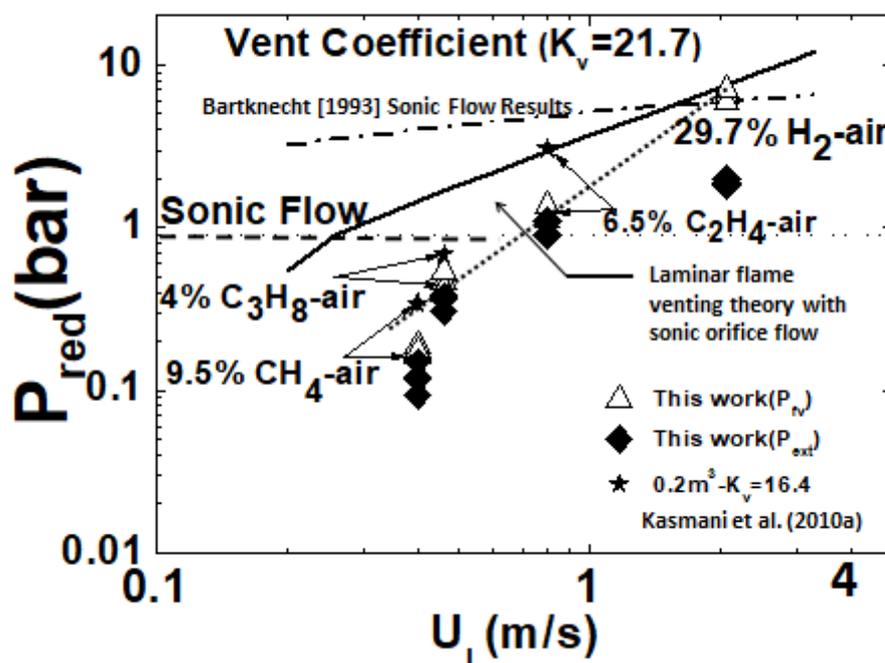
Figure 14: P_{red} as a Function of U_L for $K_v = 21.7$ with Comparison with Eqs. 6, 9 and 11.

Table 6: Experimental and Theoretical Influence of Mixture Reactivity for $K_v=21$ and $P_{stat}=0$.

Gas	U_L m/s	P_{fv} P_{red} Bar	P_{ext} bar	Normalised P_{fv}	Subsonic flow $(U_L/0.43)^2$	Sonic Flow $U_L/0.43$	Normalised K_G	Normalised Bartknecht reactivity 'a'
Methane	0.43	0.18	0.13	1	1	1	1	1
Propane	0.46	0.45	0.38	2.5	1.14	1.07	1.82	1.22
Ethylene	0.80	1.2	1.1	5.5	3.46	1.86		
Hydrogen	3.5	6.0	2.0	9	66.3	8.14	10	1.77

The vented explosion results as a function of U_L are shown in Fig. 14 for $K_v = 21.7$. Comparison with the laminar flame venting theories in Eqs. 6 and 7 (NFPA 68:2013) still over predict the experimental results, but are relatively close. The difference between Eqs. 6 and 7 the vent discharge coefficient. For methane and propane the experimental results show

12th International Symposium on Hazards, Prevention and Mitigation of Industrial Explosions
Kansas City, USA - August 12-17, 2018

XII ISHPMIE
Kansas City, MO August 12-17, 2018

subsonic venting occurred, whereas laminar flame theory predicted that sonic venting should occur. Again the difference was due to the assumption of A_s as the maximum flame area was not valid. All the overpressures were predicted to be far too high apart from hydrogen.

The over prediction of the measured P_{red} by Eq. 6 in Figs. 12 and14 could be explained by the actual flame area at the time of the peak overpressure being less than A_s. This is equivalent to reducing the assumed flame area A_s by a factor of about 3 or introducing a correction constant on the area in Eq. 9 of 0.33. For a cubic explosion vessel this reduces the C_2 constant in Eq. 9 from 6 to 2 and this is in precise agreement with the flame area constant used by Cates and Samuels (1991) based on videos of vented explosions in a Perspex vented box. Cates and Samuels (1991) found that the surface area of the flame at the position of maximum overpressure was twice the cross sectional area of the vessel and for a cubic vessel this is the same as $C_2=2$ in Eq. 9. However, the time of flame arrival data in Figs. 4 - 7 indicates that the overpressure due to turbulent flame propagation in the external vent flow is significant.

7. Conclusions

1. Free vented explosions in a small 0.01 m^3 vessel with an L/D of 2.8 were investigated, as it was considered that this size would produce a laminar flame explosion that would enable laminar flame venting theory to be validated without empirical turbulence factors. The results showed that after an initial period of flame propagation from the spark at the laminar spherical flame speed there was a fast central flame accelerating towards the vent, which left a trapped unburned gas volume in the vessel. This fast flame speed was not significantly influence by K_v and was measured well upstream of the vent and not influenced by the acceleration of the flow into the vent. It was concluded that the increased downstream flame speeds were due to the preferential expansion of the flame in the axial direction of the vent, rather than self-acceleration.

2. The form $1/K_v = a\,P_{red}^{-n}$ of the venting design equations of Bartknecht, for $P_{stat}=0.1$bar, was shown to be the same as in the Swift approach that is recognised by NFPA 68. For agreement with Bartknecht's results for methane and propane venting the laminar flame venting theory only needs a burning velocity enhancement factor of 2.60 and 2.56 respectively. The theory allows the effect of gas reactivity to be predicted. For the present 10L vented vessel, the theory over predicts the measurements for methane, propane and ethylene but is in reasonable agreement with the hydrogen results. The higher predicted values were due to the assumption of the maximum flame area being A_s and the actual flame area at the time of maximum overpressure being less than this.

3. The laminar flame venting theory is very similar to that of Bradley and Mitcheson [1978] and Swift [1983] if the same vent orifice discharge coefficient C_d is used. The adoption of the Swift [193, 1988] approach to laminar flame venting design for P_{red} up to 0.5 bar in NFPD 68 2013 is justified as it is in good agreement with the present results and with many other vented explosion results in the literature. The extension of this approach to hydrogen air venting is justified by the present results.

4. The laminar flame venting theory expanded to include self-acceleration of flames, which give an additional volume effect, is applicable to large scale explosion venting, as it accommodates the influence of vessel volume. The laminar flame theory has perfect agreement with experimental data for a 35m^3 vented vessel without any correction term and also shows agreement with other large vented vessel results. However, there is disagreement with some large vessel results and more work is needed on the vessel volume effect for constant K_v vented explosions.

12th International Symposium on Hazards, Prevention and Mitigation of Industrial Explosions
Kansas City, USA - August 12-17, 2018

XII ISHPMIE
Kansas City, MO August 12–17, 2018

5. The explosions at low K_v=4.3 showed two peaks in the overpressure, P_{fv} and P_{ext}. The overpressure due to the external explosion was higher than that due to the vent flow at low K_v, but the reverse occurred for high K_v. Also at low K_v the very reactive hydrogen explosions had sonic vent flow and the pressure loss due to unburned gas flow through the vent dominated the overpressure.

7. The Bartknecht design Equation 12 under predicts the P_{red} for hydrogen in spite of the over prediction for the other gases. In view of this, the approved EU design procedures for hydrogen explosion venting need revision and more experimental work is required on vented hydrogen explosions.

Acknowledgements

References

Andrews, G.E. and Bradley, D. (1972a) Determination of burning velocity, Combustion and Flame, 18, 133.

Andrews, G.E. and Bradley, D. (1972b) The burning velocity of methane-air mixtures, Combustion and Flame, 19, 275.

Andrews, G. E. and Bradley, D. (1973) Determination of burning velocity by double ignition in a closed vessel. Combustion and Flame, 20, 77-89.

Andrews, G. E. and Phylaktou, P. N. (2010) Handbook on Combustion (Eds. Lackner, M., Winter, F. and Agarwal, A.K.) Vol. 1, Chapter 16 Explosion Safety, 377-413: Wiley-VCH Books.

Bartknecht, W. (1993) Explosionsschultz, Grundlagen und Anwendung, Springer Verlag.

Bauwens, C.R., Chaffee, J. and Dorofeev, S. (2010) Effect of Ignition Location, Vent Size and Obstacles on Vented Explosion Overpressure in Propane-Air Mixtures. Combustion Science and Technology,182:11-12, 1915-1932.

Bimson, S.J., Bull, D.C., Cresswell, T.M., Marks, P.R., Masters, A.P., Prothero, A., Puttock, J.S., Rowson, J.J. and Samuels, B. (1993) An Experimental Study of the Physics of Gaseous Deflagrations in a Very Large Vented Enclosure. 14th International Colloquium on the Dynamics of Explosions and Reactive System, Coimbra, Portugal, Aug. 1-6, 1993.

BS1042

Bradley, D., (1997) Evolution of Flame Propagation in Large Diameter Explosions. Proc. 2nd International Seminar on Fire and Explosion Hazards, p.51-59.

Bradley, D., Cresswell, T. M. and Puttock, J. S. (2001) Flame acceleration due to flame-induced instabilities in large-scale explosions. Combustion and Flame, 124, 551-559.

Bradley, D. and Mitcheson, A. (1976) Combustion and Flame , 26, 201.

Bradley, D. and Mitcheson, A. (1978a) The venting of gaseous explosions in Spherical Vessels ! - Theory. Combustion and Flame 32, 221-236.

Bradley, D. and Mitcheson, A. (1978b) The venting of gaseous explosions in spherical vessels. II--Theory and experiment. Combustion and Flame, 32, 237-255.

Bromma (1957) Kommitten for explosionforsok.Slutrapport, Stockholm April 1958.

Buckland, I.G. (1980). Explosions of gas layers in a room size chamber. 7th Int. Symp. in Chemical Process Hazards with special reference to plant design. IChemE Symposium Series No. 58.

Cashdollar, K. L., A. Zlochower, I., Green, G. M., Thomas, R. A. and Hertzberg, M. (2000) Flammability of methane, propane, and hydrogen gases. Journal of Loss Prevention in the Process Industries, 13, 327-340.

Cates, A. and Samuels, B. A (1991) Simple Assessment Methodology for Vented Explosions. J. Loss Prev. Process Ind. Vol. 4 p. 287-296.

Catlin, C. A. (1991) Scale effects on the external combustion caused by venting of a confined explosion. Combustion and Flame, 83, 399-411.

Chippett, S. (1984) Combustion and Flame, 55, 127-140.

Cooper, M. G., Fairweather, M. and, J. P. Tite. (1986) On the mechanisms of pressure generation in vented explosions. Combustion and Flame, 65, 1-14.

Epstein, Swift, I. and Fauske (1986), Combustion and Flame, 66, 1.

En14994:2007 Gas Explosion Venting protection system. BSI.

European Parliament and Council, A. T. (1994) "The Explosive Atmosphere Directive (ATEX)" 94/9/EC. Equipment and Protective Systems Intended for Use in Potentially Explosive   Atmospheres. In: Ec (ed.) 94/9/EC. The Explosive Atmosphere Directive

Fakandu, B.M., Kasmani, R.M., Andrews, G.E. and Phylaktou, H.N. (2012). The Venting of Hydrogen-Air Explosions in an Enclosure with L/D=2.8. Proc. IX ISHMIE International Symposium on Hazardous Materials and Industrial Explosions.

Fakandu, B.M., Andrews, G.E., Phylaktou, H.N., (2014). Comparison of central and end spark position for gas explosions in vented vessels with L/D of 2.8 and 2.0. Proceedings of the Tenth International Symposium on Hazards, Prevention, and Mitigation of Industrial Explosions (XISHPMIE) Bergen, Norway, 10-14 June 2014.

Fakandu B., Mbam C., Andrews G., Phylaktou H., (2016a), Gas explosion venting: external explosion turbulent flame speeds that control the overpressure, Chemical Engineering Transactions, 53, 1-6. DOI: 10.3303/CET1653001

Fakandu, B.M., Andrews, G.E. and Phylaktou, H.N. (2016b). Gas Explosion Venting: Comparison of Experiments with Design Standards and Laminar Flame Venting Theory. Proceedings of the 11th International Symposium on Hazards, Prevention and Mitigation of Industrial Explosions, 11th ISHPMIE, Ed Wei Gao, p.1320-1332.

France, D.H. and Pritchard, R. (1977), "Burning Velocity Measurements of Multicomponent Fuel Gas Mixtures", Gas Warme International, 26, 12 .

Harris, R.J. (1983) The Investigation and Control of Gas Explosions in Buildings and Heating Plant. The British Gas Corp. Lonson:E&FN Spon.

Harris, R. J. and Wickens, M. J. (1989) Understanding Vapour Cloud Explosions – An experimental   study. Inst Gas Engineers 55th Autumn Meeting, Comm 1408.

Harrison, A.J. and Eyre, J.A. Combust. Sit. Tech. 1987, 52, 91.

Hattwig, M. and Steen, H., "Handbook of Explosion Prevention and Protection". p. 483, p.571 2004, Wiley-VCH

Hochst, S. and Leuckel, W. (1998), "On the Effect of Venting Large Vessels with Mass Intert Panels". J. Loss Prevention in the Process Industries, 11, 89-97.

Howard, W.N.(1972) Interpretation of building explosion accident. Loss prevention 6:68.

Hermanns, R. T. E., Konnov, A. A., Bastiaans, R. J. M., De Goey, L. P. H., Lucka, K. and Köhne, H. (2010) Effects of temperature and composition on the laminar burning velocity of CH4 + H2 + O2 + N2 flames. Fuel, 89, 114-121.

Hjertager, B. H. (1984) Influence of turbulence on gas explosions. Journal of Hazardous Materials, 9, 315-346.

Kasmani, R. M.; Willacy, S; Phylaktou, HN; Andrews, GE, (2006) Self accelerating gas flames in large vented explosion volumes that are not accounted for in current vent design correlations 2nd International Conference on Safety & Environment in Process Industry, Naples. Chemical Engineering Transactions, Vol. 9, p.245-250, 2006.

R.M. Kasmani , G.E. Andrews, H.N.Phylaktou, S.K. Willacy (2007), Vented Gas Explosion

12th International Symposium on Hazards, Prevention and Mitigation of Industrial Explosions
Kansas City, USA - August 12-17, 2018

XII ISHPMIE
Kansas City, MO August 12–17, 2018

in a Cylindrical Vessel with a Vent Duct. The European Combustion Institute Meeting, Chania, Crete, April, 2007.

Kasmani, R.M, Andrews, G.E., Phylaktou, H.N., Willacy, S.K. (2010a) The Influence of Vessel Volume and Equivalence Ratio of Hydrocarbon/air Mixtures in Vented Explosions Chemical Engineering Transactions, Vol.19, p.463-468.

Kasmani, R. M., Fakandu, B., Kumar, P., Andrews, G. E. and Phylaktou, H. N. (2010b) Vented Gas Explosions in Small Vessels with an L/D of 2. Proc. 6th Int. Sem. on Fire and Explosion Hazards, p.659-669. Research Publishing, ISBN-13:978-981-08-7724-8.

Kumar, R. K., Skraba, T. and Greig, D. R. (1987) Vented combustion of hydrogen-air mixtures in large volumes. Nuclear Engineering and Design, 99, 305-315.

Kumar et al. Combustion and Flame, 89, 320-332, 1992.

Molkov, V., Dobashi, R., Suzuki, M. and Hirano, T. (1999) Modeling of vented hydrogen-air deflagrations and correlations for vent sizing. Journal of Loss Prevention in the Process Industries, 12, 147-156.

Molkov, V., Dobashi, R., Suzuki, M. and Hirano, T. (2000) Venting of deflagrations: hydrocarbon-air and hydrogen-air systems. Journal of Loss Prevention in the Process Industries, 13, 397-409.

Mulpuru, S. R., Kumar , R. K. and Tamm, A. H. Prediction of pressure transient from hydrogen combustion of hydrogen combustion in a vessel. 30th Annual Meeting of the American Nuclear Society.

NFPA68 (2007). Guide for Venting of Deflagrations, NFPA 68. 2007: National Fire Protection Association.

NFPA68 (2013). Guids for Venting of Deflagrations, NFPA 68. 2013: National Fire Protection Association.

Pappas, J.A. and Foyn, T. (1983). Gas Explosion Research Programme. Final Report 83-1334, Det Norsk Veritas, 1983. (Data given in Cates, A. and Samuels, B. (1991) A simple Assessment Methodology for Vented Explosions. J. Loss Prev.Process Ind., Vol.4 p.287-296, 1991.)

Phylaktou, H. and Andrews, A. G. E. (1990) Gas Explosions in Long Closed Vessels. Combustion Sceince and Technology, 1-3, 27-39.

Phylaktou, H.N. and Andrews, G.E. (1991) The acceleration of flame propagation in a tube by an obstacle. Combustion and Flame, Vol.85, pp.363-379.

Phylaktou, H. and Andrews, G. E. (1993) Gas explosions in linked vessels. Journal of Loss Prevention in the Process Industries, 6, 15-19.

Razus, D. M. and Krause, U. (2001) Comparison of empirical and semi-empirical calculation methods for venting of gas explosions. Fire Safety Journal, 36, 1-23.

Runes, E. (1972) Explosion venting in Loss Prevention. Proceedings of the 6th Symposium on Loss Prevention in the Chemical Industry New York.

Sato, K, Tano, S. and Maeda, Y. (2010) Observations of Venting Exlosions in a Small Cubic Vessel with Rich Propane-Air Mixtures. Proc. Sixth Int. Sem on Fire and Explosion Hazards. p.671-682. Research Publications, ISBN 978-981-08-7724-8. doi:10.3850/978-981-08-7724-8_10-03

Sattar, H., Andrews, G.E., Phylaktou, H.N, and Gibbs, B.M., 2014, Turbulent flame speeds and laminar burning velocities of dusts using the ISO 1 m^3 dust explosion method. Chemical Engineering Transactions, 36, 157-162. DOI: 10.3303/CET1436027.

Siwek, R. (1996) Explosion venting technology. Journal of Loss Prevention in the Process Industries, 9, 81-90.

12th International Symposium on Hazards, Prevention and Mitigation of Industrial Explosions
Kansas City, USA - August 12-17, 2018

XII ISHPMIE
Kansas City, MO August 12–17, 2018

Solberg, D. M., Pappas, J. A. & Skramstad, E. (1980) Observations of flame instabilities in large scale vented gas explosions. 18th International Symposium on Combustion. The Combustion Institute.

Solberg, D. M., Pappas, J. A. & Skramstad, E. (1980) Experimental explosion of part confined explosion. Analysis of pressure loads, Part 1. Det Norske Veritas Research Division Technical Report no 79-0483.

Swift, I. (1988) Design of deflagration protection systems. Journal of Loss Prevention in the Process Industries, 1**,** 5-15.

Swift, I. (1989) NFPA 68 guide for venting of deflagrations: what's new and how it affects you. Journal of Loss Prevention in the Process Industries, 2**,** 5-15.

Taylor, G.I., (1946). The air wave surrounding an expanding sphere.Proc. Royal Soc. A180,273.

Tomlin, G. and Johnson, D.M. (2013). A Large Scale Study of the Venting of Confined Explosions into Unobstructed and Congested Flammable Vapour Clouds. Proc. 7th Int. Sem. Fire and Explosion Hazards (ISFEH7), pp,679-688. Eds. D. Bradley, G. Makhviladze, V. Molkov, P. Sunderland and F. Tamanini, Research Publishing.

Yao, C. (1974) Explosion venting of low-strength and structures. Loss prevention, 8**,** 1-9.